

# Biomechanical Simulation of the Vitreous Humor in the Eye Using an Enhanced ChainMail Algorithm

Markus A. Schill<sup>1,2,3</sup>, Sarah F. F. Gibson<sup>1</sup>, H.-J. Bender<sup>3</sup>, and R. Männer<sup>2</sup>

<sup>1</sup> MERL – A Mitsubishi Electric Research Laboratory, 201 Broadway, Cambridge, MA, 02139, USA, <http://www.merl.com>

<sup>2</sup> Lehrstuhl für Informatik V, Universität Mannheim, B6, D-68131 Mannheim, Germany, <http://www-mp.informatik.uni-mannheim.de>

<sup>3</sup> Institut für Anästhesiologie und Operative Intensivmedizin, Fakultät für klinische Medizin Mannheim der Universität Heidelberg, D-68135 Mannheim, Germany  
[markus.schill@ti.uni-mannheim.de](mailto:markus.schill@ti.uni-mannheim.de) [gibson@merl.com](mailto:gibson@merl.com)

**Abstract** The focus of this paper is the newly developed Enhanced ChainMail Algorithm that will be used for modeling the vitreous humor in the eye during surgical simulation. The simulator incorporates both visualization and biomechanical modeling of a vitrectomy, an intra-ocular surgical procedure for removing the vitreous humor. The Enhanced ChainMail algorithm extends the capabilities of an existing algorithm for modeling deformable tissue, 3D ChainMail, by enabling the modeling of inhomogeneous material. In this paper, we present the enhanced algorithm and demonstrate its capabilities in 2D.

## Introduction

A vitrectomy removes the vitreous humor, a gelatinous substance filling the eyeball (see Figure 1). This procedure is performed under numerous pathological conditions, including an opaque vitreous body or traction ablatio, where thin pathological membranes and tissue fibers on the retina contract and start to lift the retina from the sclera. In the case of an opaque vitreous body, the vitreous humor is removed and replaced with a clear fluid. To address traction ablatio, the vitreous humor is first removed to allow access to the pathological membranes.

During the vitrectomy, two narrow instruments are inserted into the eye – a vitrector and a cold light lamp. The vitrector has a hole at the side of its tip through which material is sucked in and extracted with an internal oscillating knife. The extracted material is then pumped out through the handle of the vitrector. The cold light lamp is used to generate reflections on the surface of the otherwise highly transparent vitreous humor, helping the surgeon to visualize remaining material. The lamp also casts a strong shadow of the instrument onto the retina. This shadow provides depth cues to the surgeon, an important means for estimating the distance between the instrument and the highly sensitive retina.

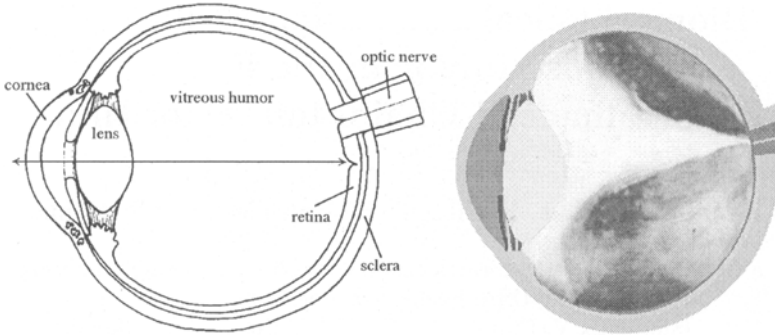


**Figure 1.** The EyeSi project will simulate removal of the vitreous humor from the eyeball. (Left) A diagram of the eye. (Right) Pathological vitreous humor. For this picture a photography and a 2D model were superposed.

A collision between the vitrector and the retina can result in loss of eye sight. Unfortunately, because vitrectomies are performed using a stereo microscope, hand-eye coordination can be extremely difficult within the small volume of the eye (the eye's diameter is 2.6 cm). These constraints, in addition to a lack of well-defined mechanical feedback from motion of the instruments, mean that vitrectomies are challenging both to perform and to teach. To address the need for better teaching tools, the University of Mannheim has begun the EyeSi project, a computer-based simulator for intra-ocular surgery.

### The EyeSi Project

The EyeSi project aims to develop a computer-based training workstation for the simulation of a vitrectomy, the removal of the vitreous humor from the eyeball. The simulator is designed to augment the training and rehearsal of intra-ocular surgery. The project addresses both navigation inside the eye and the removal of the vitreous humor with a vitrector. During the simulation, the user manipulates a vitrector and a cold light lamp. The positions of these two instruments are tracked by an optical tracking system<sup>1</sup> and monitored by a PC-based workstation. The instrument positions are used to render the instruments in a graphical representation of the computer eye model and to detect possible interactions with the vitreous humor. Because the vitreous humor is an inhomogeneous, semi-transparent, highly deformable gel, the system uses a volumetric representation (rather than a surface-based representation) for modeling and visualization of this substance.

<sup>1</sup> The tracking system uses i-cam, an intelligent camera system developed by the Fachhochschule für Technik, Mannheim. Each CCD camera is equipped with a digital signal processor (DSP) which can be programmed to perform simple image processing tasks and position tracking. Using the DSPs for motion prediction is planned for the future.

EyeSi will use a volume rendering system developed at the Lehrstuhl für Informatik V, Universität Mannheim<sup>2</sup> which provides combined visualization of volume and surface objects and shadow casting [4], [7]. As described above, rendering shadows is particularly important for providing depth cues to the surgeon to help avoid damaging the retina with the vitrector tip. The system will combine surface-based object representations for the surgical instrument and the outer geometry of the eyeball with a volumetric representation of the vitreous humor (Figure 1 (right) shows a 2D model). The biomechanical behavior of the volumetric vitreous humor will be simulated with the Enhanced ChainMail Algorithm presented in this paper. The enhancement allows the modeling and deformation of inhomogeneous volumetric material at interactive rates.

## Recent Work on Eye Surgery Simulation

The structure and function of the human eye are well understood. This together with its spherically symmetric shape and its relatively simple structure on one hand, and its high sensitivity and fragility on the other hand make it a good candidate for surgical simulation.

A number of others have developed computer based simulations of the eye for education and training. For example, the Biomedical Visualization laboratory at the University of Illinois have developed an anatomical atlas of the eye [1]. Most systems that have been developed for simulating eye surgery deal with structures, such as cataracts, that are on or near the surface of the eye. Hence, these systems use surface-based object representations and surface rendering (e.g. [6], [5]). In these systems, interactions with surgical instruments have been modeled using Finite Element Methods, where either on-line computation limits the rates of interactions with the object models [6] or off-line calculations or the incorporation of previously measured interaction forces limit the flexibility of the system [5].

## The Enhanced ChainMail Algorithm

Because of the highly deformable nature of the vitreous humor and the mechanical complexity of the extraction process, the surgical procedure is not well modeled with conventional deformation techniques such as mass-spring systems or Finite Element Methods. Solving Navier Stokes based 3D computational fluid dynamics for this problem can not be performed at the required update rates. While particle systems provide a possible solution [2], the lack of direct inter-particle communication can also make these systems too slow for an interactive simulation when a relatively large number of particles are used. In contrast, the 3D ChainMail algorithm, introduced by Gibson in 1997 [3], provides fast interactions with highly deformable materials containing 10's of thousands of elements.

---

<sup>2</sup> <http://www-mp.informatik.uni-mannheim.de/research/VIRIM>

This capability provides the potential for addressing the highly demanding requirements of the EyeSi project. However, 3D ChainMail has a number of limitations. In the rest of this paper, we outline the capabilities and limitations of 3D ChainMail and introduce an Enhanced ChainMail Algorithm that addresses some of these limitations. The features of this new algorithm are defined and illustrated in 2D.

**3D Chainmail:** 3D ChainMail is the first step in an iterative process that models shape changes in deformable objects. Its function is to approximate the new shape of a deformed object by minimally adjusting element positions to satisfy geometric constraints between the elements in the volumetric object. The second step in the deformation process, Elastic Relaxation, relaxes the approximate shape of a deformed object to reduce an elastic energy measure in the object.

3D ChainMail is physically-based in the sense that the information of a deformation process is propagated through the object by passing it from one volume element to another. As information travels through the object, each element reacts by adjusting its own position within certain material constraints. By adjusting its position, an element changes the information (the amount of deformation still to be performed) that is propagated to neighboring elements. Once this deformation information is reduced to zero or there are no more neighbors to propagate the information to, the process ends. Fig. 2 illustrates the ChainMail process in one dimension.

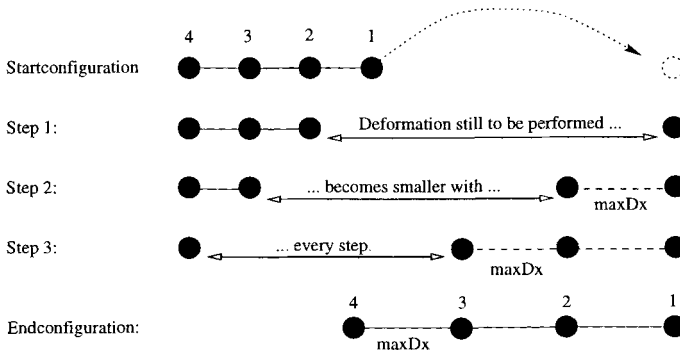


**Figure 2.** The deformation is initiated by moving element #1. In the next step, element #2 implicitly changes the information that is passed on to element #3 by adjusting its position according to the material constraint,  $\max D_x$ , where  $\max D_x$  is the maximum allowed distance between two elements. When the original elements are separated by a distance less than  $\max D_x$ , the amount of deformation that remains to be performed decreases with every step

The ChainMail algorithm enables fast propagation of the deformation information because connections to neighboring elements are explicitly stored in the

object data structure. The algorithm described in [3] uses 4-connected neighborhoods in 2D and 6-connected neighborhoods in 3D. The relative positions between neighboring elements are governed by a set of deformation and shear constraints. Figure 3 shows the six constraints that determine the material properties in 2D. Different constraints controlling vertical, horizontal, and front-to-

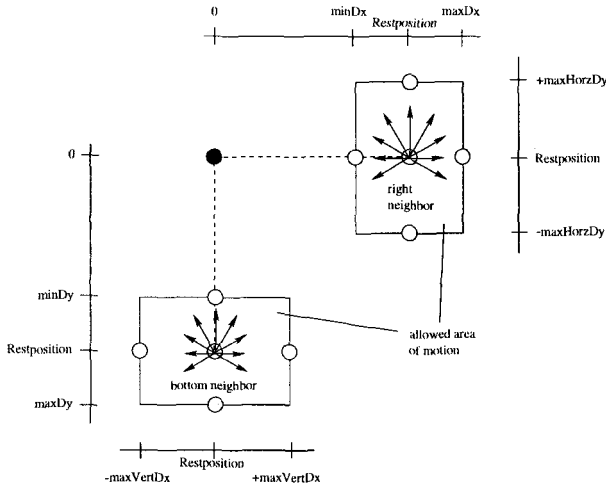


**Figure 3.** The geometric constraints between an element (black) and its right and bottom neighbors are illustrated. In 2D, six material constraints are used to model different material properties with ChainMail:  $\max Dx$ ,  $\min Dx$ ,  $\max Dy$ , and  $\min Dy$  govern the compression or stretch of the material, while  $\max VertDx$  and  $\max HorzDy$  govern the possible shear between neighbors.

back deformation and shear allow anisotropic material properties. However, the algorithm is particularly fast because it assumes that these constraints are constant throughout the volumetric object. Because the vitreous humor is not homogeneous, especially in pathological cases, it is important that we expand the algorithm presented in [3] to address inhomogeneous tissues.

**Enhanced ChainMail:** For inhomogeneous materials, the first-moved-first-processed element processing order that was used in 3D ChainMail is no longer appropriate. As expected, a straightforward application of ChainMail using this processing order gave inconsistent deformations for inhomogeneous materials that resulted in holes and tears. The Enhanced ChainMail algorithm addresses this problem with a new element processing order.

Refining the ChainMail algorithm for inhomogeneous materials required thinking about deformation as a physical process in which deformation information travels through the material as a sound wave. In general, the speed of sound is higher in denser material because the “connection” between elements is stiffer. In

ChainMail the “stiffness” of a connection between two neighbors is determined by the material constraints of the two elements. In inhomogeneous materials, when neighboring elements have different material constraints, the constraints for the link between the two neighbors are calculated using contributions from both elements. Fig. 4 shows the constraints that are assigned to a single element in the enhanced ChainMail algorithm and Fig. 5 illustrates how the two neighbors contribute to the constraints that determine their relative behavior.

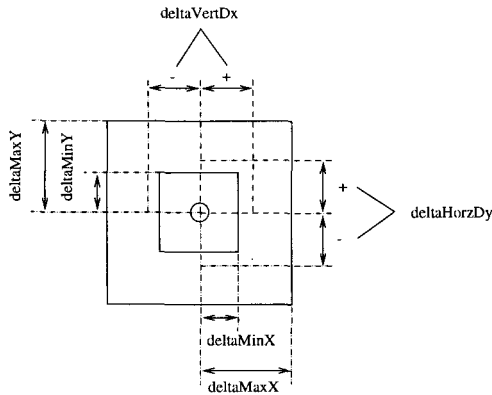


**Figure4.** Constraints assigned to a single element in the Enhanced ChainMail Algorithm.  $\text{deltaMaxX}$ ,  $\text{deltaMinX}$ ,  $\text{deltaMaxY}$ , and  $\text{deltaMinY}$ , correspond to maximum allowed stretch and compression in the horizontal and vertical directions respectively.  $\pm\text{deltaVertX}$  and  $\pm\text{deltaHorzY}$  correspond to the maximum allowed shear to vertical and horizontal neighbors respectively.

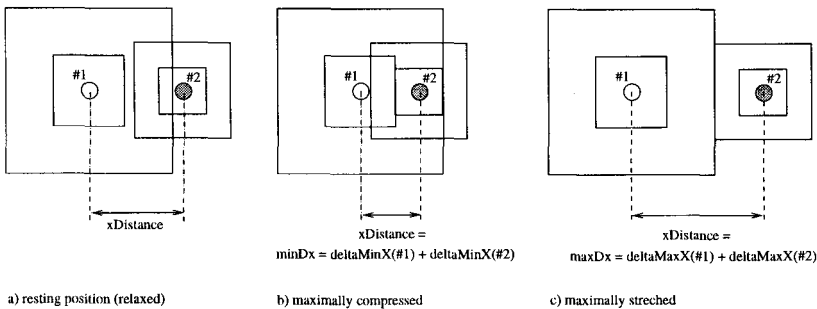


**Figure5.** The contributions of both neighbors combine to give the constraints that govern the link between them.

The order in which neighbors of a moved element are processed determines where the deformation information is propagated first. Hence, the processing

order can be used to model material and direction-dependent propagation speeds in the object. The Enhanced ChainMail Algorithm uses this observation to order the processing of elements in the object so that the deformation travels most quickly through stiff materials. The ordering is determined by comparing the constraint violations between neighboring elements and processing elements with the largest constraint violations first. For example, the constraint violations for element #2 in step 1 of Fig. 2 is determined as follows:

$$\text{amount of constraint violation} = \text{distance}_{\#1, \#2} - \max D\alpha$$

After moving an element, its neighbors are examined to determine whether any constraint has been violated. If so, the neighbor with the largest constraint violation is processed first. This is equivalent to processing neighbors in the order in which their constraints were violated, guaranteeing that the deformation information is propagated fastest through stiff materials.

### Algorithm outline

The Enhanced ChainMail Algorithm maintains an ordered list of elements that must be considered for a movement. The ordering criteria for the list is the size of the constraint violation. The process starts when an initial sponsoring element in the object is moved to a new position. After this, neighboring elements are inserted into the list, whereby the previous ordering principle is maintained, according to which the element with the largest constraint violation is always at the head of the list. Next the first element is popped from the list and moved to satisfy the constraint against its sponsor. (The sponsor is the element by whose movement the current element was added to the list.) The process ends when the list is exhausted. The following is pseudo code for the Enhanced ChainMail Algorithm:

```
initialSponsor.position = newPosition ;
insertNeighborsToList(initialSponsor) ;
while (elements in lists)
    popFirstElementFromList ;
    if(checkVsSponsor demands move)
        thisElement.updatePosition ;
        addNeighborsToList(thisElement) ;
```

The candidate list can be sorted easily if new elements are inserted into the correct position when they are added to the list. Currently the list is implemented as a binary tree, making it relatively fast and easy to insert and find elements. However element insertion is the most time-consuming process in the current implementation.

### Results

To model inhomogeneous material with ChainMail the first-moved-first-processed criteria used for homogeneous materials is no longer valid. It must be replaced

by the more general principle first-“violation of constraint”-first-processed. The Enhanced ChainMail Algorithm was implemented and tested in 2D for a number of test objects and integrated into a general system which enables a 2D gray-scale image to be read into the system, material constraints to be set using a lookup table on gray-scale values, and the resultant 2D model to be interactively manipulated. The sequence in Figure 6 shows the deformation of a gray-scale picture using this system. The gray values in the original picture (top, left) were mapped to material constraints that were a linear function of the gray scale value, where black pixels became rigid elements and white pixels became highly deformable elements. The sequence shows the deformation of the image when an element on the right side of the image is grabbed and moved to the right. Notice how the more rigid hair on the left border of the picture affects the softer surrounding material during the deformation.

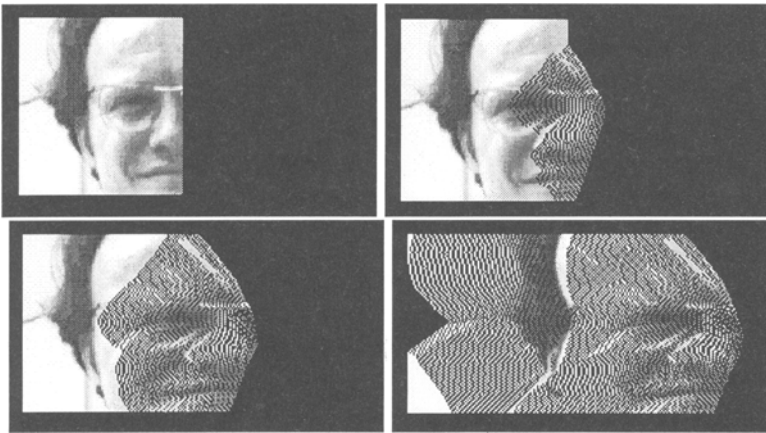


**Figure 6.** The gray values of the original picture (top left) are interpreted as material constraints. White is soft and black is rigid material.

Because of the sorting required for determining the processing order of object elements, the Enhanced ChainMail algorithm is slower than the original 3D ChainMail algorithm. However, we were able to achieve interactive rates for deforming a  $100 \times 100$  inhomogeneous image. The system was implemented in C++ on a PC with a Pentium 200 MHz processor.

## Discussion

The Enhanced ChainMail algorithm addresses the need for modeling complex, inhomogeneous materials at interactive rates in simulations such as modeling the vitreous humor in the EyeSi project. The algorithm will be used in the EyeSi



Project but is also well suited for other tissue modeling applications. While the results and analysis presented here were limited to 2D, extension to 3D is straightforward.

While this work has demonstrated that the algorithm presented here will make simulation of the vitreous humor feasible, there are a number of important areas of future work. First, speed of the algorithm must be improved. For this reason, we have begun investigating parallelizing the Enhanced ChainMail algorithm. Because the algorithm considers  $x$ ,  $y$ , and  $z$  displacements independently and the resultant deformation is a superposition of the solutions along these three axes, the system can easily be parallelized by calculating deformations along the  $x$ ,  $y$ , and  $z$  axes on different processors.

Two additional limitations of the current Enhanced ChainMail Algorithm are that it does not model volume conservation, an important characteristic of many tissues in the human body, and that, because of the axis-aligned material constraints, it does not model inter-element rotation. There are at least two ways to impose volume conservation on the deforming volume. The first is to incorporate volume conservation into the Elastic Relaxation step of the two-process deformation system described above. The second is to change material constraints along the axes perpendicular to the deformation axis according to constraint violations in the direction of deformation. We have implemented this second approach in a test system with promising results. We have also begun investigating the addition of a new degree of freedom to indicate element orientation so that inter-element rotation can be modeled.

## References

1. Biomedical Visualization Laboratory at University of Illinois. Model of the Eye. <http://www.bvl.uic.edu/bvl/eye/>.
2. M. Desbrun and M-P. Gascuel. Animating Soft Substances with Implicit Surfaces. In *SIGGRAPH '95*, pages 287 – 290, Los Angeles, CA, USA, 1995.
3. S. Gibson. 3D ChainMail: A Fast Algorithm for Deforming Volumetric Objects. In *1997 Symposium on Interactive 3D Graphics*, pages 149 – 154, Providence, RI, USA, April 1997.
4. A. Gröpl, T. Günther, J. Hesser, J. Kröll, R. Männer, C. Poliwoda, and C. Reinhart. Interactive Operation Planning and Control with VIRIM. In *Proc. Medicine Meets Virtual Reality 4*, pages 121–133, San Diego, CA, January 1996.
5. Medical College of Georgia & IMTC at GeorgiaTech. Simulation of a Catheract Surgery. <http://www.oip.gatech.edu/MMTLPROJ/eye.html>.
6. Mark A. Sagar, David Bullivant, Gordon D. Mallinson, and Peter J. Hunter. A Virtual Environment and Model of the Eye for Surgical Simulation. In *SIGGRAPH '94*, Annual Conference Series, pages 205–212, July 1994.
7. M. Schill, Ch. Reinhart, T. Günther, Ch. Poliwoda, J. Hesser, M. Schinkmann, H.-J. Bender, and R. Männer. Biomechanical Simulation of Brain Tissue and Real-time Volume Visualisation. Integrating Biomechanical Simulations into the VIRIM System. In *Proceedings of the international Symposium on Computer and Communication Systems for Imageguided Diagnosis and Therapy, Computer Assisted Radiology*, pages 283–288, Berlin, Germany, June 1997.